Scanning tunneling microscopy on unpinned GaN(1$\bar{1}$00) surfaces: Invisibility of valence-band states

Ph. Ebert,[1,*] L. Ivanova,[2] and H. Eisele[2]
[1]*Institut für Festkörperforschung, Forschungszentrum Jülich GmbH, 52425 Jülich, Germany*
[2]*Institut für Festkörperphysik, Technische Universität Berlin, Hardenbergstr. 36, 10623 Berlin, Germany*
(Received 25 February 2009; published 24 August 2009)

We investigated the origins of the tunnel current in scanning tunneling microscopy (STM) and spectroscopy experiments on GaN(1$\bar{1}$00) surfaces. By calculating the tunnel currents in the presence of a tip-induced band bending for unpinned *n*-type GaN(1$\bar{1}$00) surfaces, we demonstrate that only conduction-band states are observed at positive and negative voltage polarities independent of the doping concentration. Valence-band states remain undetectable because tunneling out of the electron-accumulation zone in conduction-band states dominates by four orders of magnitude. As a result band-gap sizes cannot be determined by STM on unpinned GaN(1$\bar{1}$00) surfaces. Appropriate band-edge positions and gap sizes can be determined on pinned surfaces.

DOI: 10.1103/PhysRevB.80.085316 PACS number(s): 73.20.At, 68.37.Ef

I. INTRODUCTION

Besides its atomic resolution, one of the most valuable properties of scanning tunneling microscopy (STM) and spectroscopy (STS) is the ability to probe simultaneously the filled *and* empty density of states at surfaces.[1] Depending on the polarity of the bias voltage, electrons tunnel from the filled states of the sample into empty tip states (negative sample voltage) or in opposite direction from filled tip states into empty sample states (positive sample voltages). This is the basis for all interpretations of STM and STS data and thereby also the foundation to unravel the physics behind it. One particularly illustrative manifestation of this principle for the case of semiconductors is the selective imaging of As and Ga atoms on the GaAs(110) surface,[2] arising from filled and empty dangling bonds localized above the surface As and Ga atoms, respectively. This "atom-selective imaging" combined with the fact that (110) surfaces of GaAs and other III–V compound semiconductors provide perfect cross-sectional cleavage surfaces, made the so-called cross-sectional STM one of the most successful tools to investigate the atomic and electronic properties of defects, interfaces, epitaxial layers, and buried nanostructures with atomic resolution and thereby helped to unravel the processes acting during epitaxy of III-V semiconductor devices.[3–5] The principle of voltage-dependent tunneling suggests that it is always possible to image the filled and empty density of states of a sample, as assumed in general when interpreting scanning tunneling microscopy and spectroscopy measurements.

Here, we show that in STM measurements of unpinned nonpolar *n*-type GaN(1$\bar{1}$00) surfaces the filled valence-band states, constituted primarily by the filled dangling bonds above the surface N atoms, remain always invisible. Our calculations illustrate that the tunneling current at, both, negative and positive sample voltage originates from the conduction-band states, which are primarily composed of the empty dangling bonds above the Ga atoms. Thus, the general assumption that STM always probes the complete (filled and empty) density of states at the surface, independent of its occupation, needs to be reassessed for unpinned nonpolar GaN(1$\bar{1}$00) surfaces.

The principle is illustrated here on nonpolar GaN surfaces because the detrimental electric fields caused by piezoelectricity and spontaneous polarization in this material of choice for blue and ultraviolet light-emitting devices can be removed by growth on such nonpolar surfaces.[6] This lead to a strongly increased interest in the properties of the GaN(1$\bar{1}$00) surface, which also has perfect geometric and electronic properties for cross-sectional STM of GaN epitaxial layers.[7,8] However, the invisibility of valence-band states can be expected to occur in STM measurements of many other primarily wideband-gap semiconductor materials, too, and need to be taken into account when extracting the physics of such materials.

II. THEORETICAL BACKGROUND AND DETAILS OF THE CALCULATION

For the calculation of the tunnel current, we briefly introduce the physical effects, which need to be taken into account. First, the high electric field between the tip and the sample typically penetrates into semiconductors due to the limited free charge-carrier concentration and the thereby resulting reduced screening ability.[9] This induces a so-called "tip-induced band bending," i.e., screening charges accumulate near the surface and as a result the band edges are bend downward or upward, depending on the polarity of the voltage applied to the sample relative to the tip. Only with extremely high free charge-carrier concentrations at or near the semiconductor surface the electric field induced by the applied voltage between the tip and the sample can be screened fast enough at the sample surface to avoid a penetration of the electric field into the semiconductor and thus a band bending. This is, however, only achievable by either extreme and rather unrealistic doping levels or by an intrinsic or defect state in the band gap at the surface. The later results in a so-called *pinned* surface, where the Fermi level is pinned at the energy position of the surface state. Without surface states in the fundamental band gap the bands can freely shift relative to the Fermi energy and the surface is called *unpinned*. If no STM tip is present, the energy positions of the

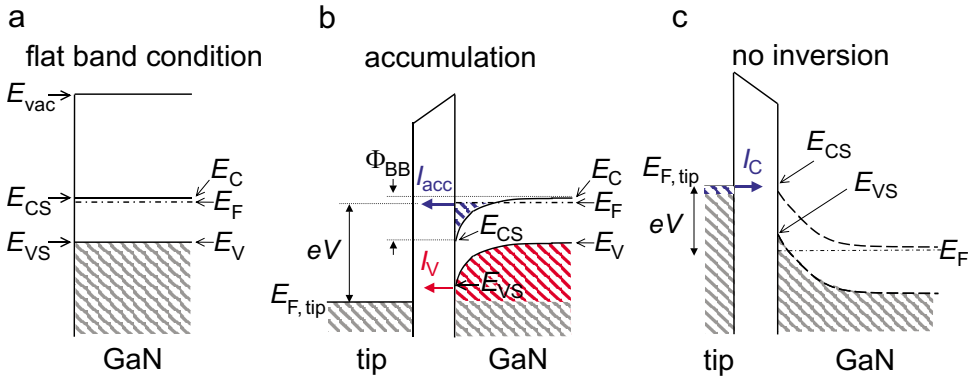

FIG. 1. (Color online) Schematic of the bending of the conduction-band (E_C) and valence-band (E_V) edges and the resulting electron occupation in the presence of a tip. (a) Flat band conditions in the absence of a metallic tip. The energy positions of the conduction-band (E_{CS}) and valence-band (E_{VS}) edges at the surface are identical with those in the bulk (E_C, E_V). No surface states are present within the fundamental band gap. (b) Electron accumulation at negative sample voltages in the conduction band. (c) Situation at positive sample voltages without carrier inversion. I_V, I_C, and I_{acc} denote the different tunnel current contributions.

band edges at the unpinned semiconductor surface are unchanged compared with those in the bulk. This is the so-called flat band condition [see, e.g., Fig. 1(a), the case of a *n*-type semiconductor]. Experimentally it has been found that no intrinsic surface states exist in the fundamental band gap for GaN($1\bar{1}00$) surfaces.[7] Thus, defect-free GaN($1\bar{1}00$) surfaces are unpinned. Pinning is only due to high defect concentrations. Therefore, we first concentrate on unpinned surfaces.

Second, the presence of a tip-induced band bending can modify significantly the electron occupation of the states at the surface. For a sufficiently large downward band bending at negative voltages the conduction-band states get filled by electrons as soon as the conduction-band minimum is dragged below the Fermi energy [Fig. 1(b)]. Under such conditions, not only electrons from the valence-band states (I_V) but also from the filled conduction-band states tunnel into empty tip states (called accumulation current, I_{acc}). As a result, one would image both valence-band and conduction-band states [i.e., As- and Ga-derived dangling bonds in case of the GaAs(110) surface]. However, in case of GaAs(110), the tunnel current I_{acc} out of the conduction-band states (Ga dangling bonds) is suppressed by the momentum conservation of the tunneling electrons:[10] the surface conduction-band minimum is at the edge of the Brillouin zone and thus the tunneling electrons have a nonzero momentum, which typically cannot be accommodated for in the density of states of the tip. Thus, under the assumption of elastic tunneling with momentum conservation as the most probable process, the electrons in the filled conduction-band states do not contribute with sufficient probability and I_{acc} in Fig. 1(b) can be neglected because the current I_V from the valence band (i.e., As dangling bonds) is dominant. Therefore, for compound semiconductor cleavage surfaces with an *indirect surface band gap* (surface conduction-band minimum not at $\bar{\Gamma}$ point), such as most zinc-blende III–V compound semiconductors,[11] anions (filled dangling bonds) and cations (empty dangling bonds) can be imaged selectively.

In contrast, nonpolar GaN($1\bar{1}00$) surfaces exhibit a *direct* surface band gap at the $\bar{\Gamma}$ point.[7,12] In order to unravel, which density of states contribute to the tunnel current on nonpolar GaN surfaces, we investigated theoretically the tunneling on *n*-type GaN($1\bar{1}00$) surfaces. Since the intrinsic surface states are outside the fundamental band gap,[7] we considered surfaces free of defects and thus unpinned as well as surfaces pinned by defects. We calculated (i) the penetration of the electric field into the GaN substrate and the resulting valence-band and conduction-band edge positions at the surface and (ii) the transmission probability for the different possible tunneling processes and the respective tunneling currents.

We based our calculation of the positions of the conduction-band (E_{CS}) and valence-band edges (E_{VS}) at the GaN($1\bar{1}00$) surface on the one-dimensional integration of Poisson's equation described by Feenstra and Stroscio[9] and Seiwatz and Green,[13] but extended it in order to include Fermi-Dirac statistics and the effects of carrier dynamics as described in Ref. 10. Therefore, carrier inversion does not occur under tunneling conditions on GaN($1\bar{1}00$), in analogy to GaAs(110).[10,14] The tunneling current is computed following Feenstra and Stroscio[9] and Bono and Good.[15] This model is based on the approach by Tersoff-Hamann[1] and Selloni *et al.*[16] to integrate over all states between the tip and the sample Fermi-level times the transmission coefficient. Parabolic bands are assumed for the density of valence-band and conduction-band states. The transmission coefficient through the vacuum barrier as well as through the semiconductor's space-charge region is estimated using the WKB approximation. Thereby the vacuum barrier is taken as trapezoidal modified by the image charge lowering.

Our calculations were performed for *n*-doped GaN with carrier concentrations of 3×10^{18}–1×10^{20} cm^{-3}. In all cases we assumed a background acceptor concentration of 3×10^{15} cm^{-3} to simulate growth impurities, a work function of 4.5 eV for the metallic tip, a tip-sample separation of 0.9 nm, and a tunneling area of 1 nm^2. A variation in these parameters does not change the results qualitatively.

III. RESULTS AND DISCUSSION

Figure 2 shows the calculated band bending at differently doped unpinned *n*-type GaN($1\bar{1}00$) surfaces underneath the

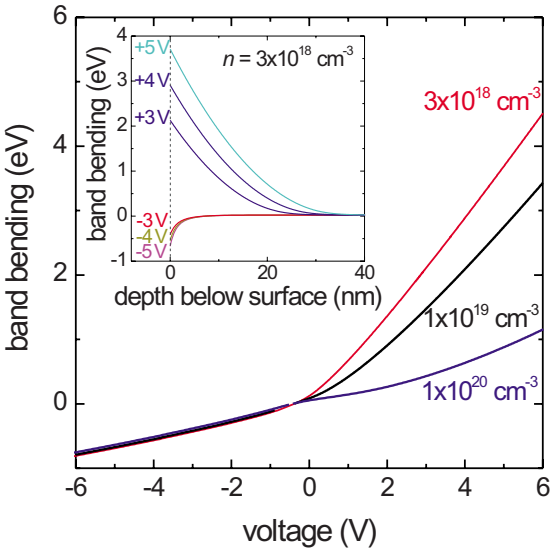

FIG. 2. (Color online) Calculated band bending at the unpinned n-type GaN surface as a function of the sample voltage for three different carrier concentrations indicated on the right side of each curve. The calculation based on a metal–vacuum–GaN system assumed that due to carrier dynamics no inversion can persist. Only accumulation of majority carriers occurs. Inset: band bending as a function of the depth for different selected voltages. The carrier concentration used for this set is 3×10^{18} cm^{-3}. The surface is at the depth 0.

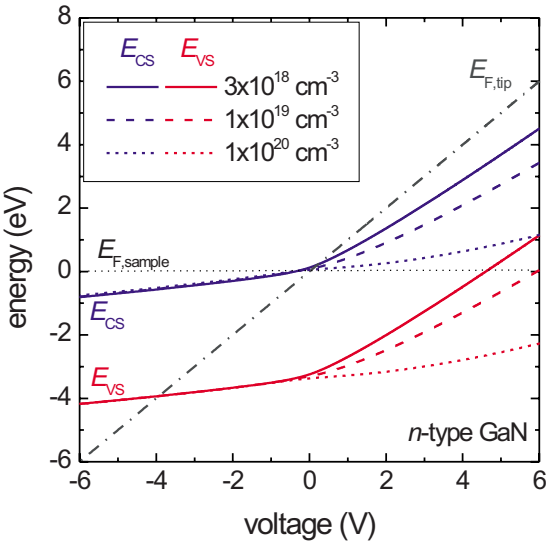

FIG. 3. (Color online) Calculation of the conduction-band (marked E_{CS}) and valence-band (marked E_{VS}) edge energies at the unpinned GaN surface as a function of the applied sample voltage. The band-edge positions are shown for three different doping levels (shown as solid, dashed, and dotted pairs of lines, respectively). The upper and lower solid, dashed, and dotted lines of these pairs of lines represent the conduction-band (marked E_{CS}) and valence-band (marked E_{VS}) edge energies, respectively. The Fermi level of the tip ($E_{F,tip}$) lies on the dashed-dotted gray diagonal line. All energies are given relative to the Fermi level of the sample (at 0 eV).

STM tip. It is obvious that independent of the carrier concentration, the tip-induced band bending cannot be neglected. It reaches especially at positive voltages V values almost as high as $e\cdot V$ with e being the electron charge. The band bending at positive voltages is primarily determined by the doping concentration. It decreases with increasing doping concentration because the screening of the electric field between the tip and the sample is achieved by the free charge-carrier concentration [see schematic in Fig. 1(c)]. At negative voltages the band bending is independent of the doping concentration. Here the screening of the electric field is arising from electrons filling the conduction-band states, as shown schematically in Fig. 1(b). The number of screening electrons at the surface depends then on the conduction-band density of states and not on the doping concentration, in analogy to the hole accumulation in the valence band described for differently p-doped GaAs(110) in Ref. 17. The different screening origin can also be recognized in the depth dependence of the band bending shown in the inset of Fig. 2. At positive voltages a deep field penetration of up to 35 nm occurs while at negative voltages the field is already fully screened after about 10 nm. This reflects the much higher density of states in the conduction band filled by electrons [majority-carrier (electron) accumulation zone screening at negative voltages as illustrated in Fig. 1(b)] as compared to the doping-induced carrier concentration screening at positive voltages [as illustrated in Fig. 1(c)].

For the further discussion we recall, that at positive (negative) voltages, a flow of tunnel current requires that the tip's occupied (empty) states must energetically face the empty (filled) states of the sample. This requirement is nontrivial for semiconductors because of the band gap and the presence of the tip-induced band bending. Without any tip-induced band-bending current-voltage spectroscopy would exhibit at negative voltages current arising from the sample's filled valence-band states and at positive voltages current due to electrons tunneling into the empty conduction-band states. The region in between with no current should then have a width in voltage reflecting the band-gap energy. In order to illustrate the situation with the strong tip-induced band bending found for GaN($1\bar{1}00$) (see Fig. 2), we determined the energy positions of the valence- (E_{VS}) and conduction-band (E_{CS}) edges at the surface underneath the tip and of the Fermi level of the tip ($E_{F,trip}$) relative to $E_{F,sample}\equiv E_F\equiv 0$ (horizontal black dotted line in Fig. 3). The Fermi level of the metallic tip is shown as a gray dashed-dotted line in Fig. 3. It lies in the GaN band gap at the surface for tunneling voltages between −3.9 V and +0.1 V for the highest-doped or +0.3 V for the lowest-doped sample. Thus in this voltage range neither electron can tunnel from the valence band into empty tip states or from filled tip states into empty conduction-band states because filled (empty) tip states do not face empty (filled) sample states. Tunneling out of valence-band states is only possible for voltages $V<$ −3.9 V. In analogy tunneling into empty conduction-band states is only possible for voltages larger than +0.1 to +0.3 V, depending on the doping level of the GaN samples. One could thus expect that a voltage region of 4.0–4.2 V wide would be without tunnel current, reflecting the GaN band gap of $E_{gap}=3.4$ V.

However, there is an additional effect. The conduction-band minimum at the surface E_{CS} is dragged to negative-

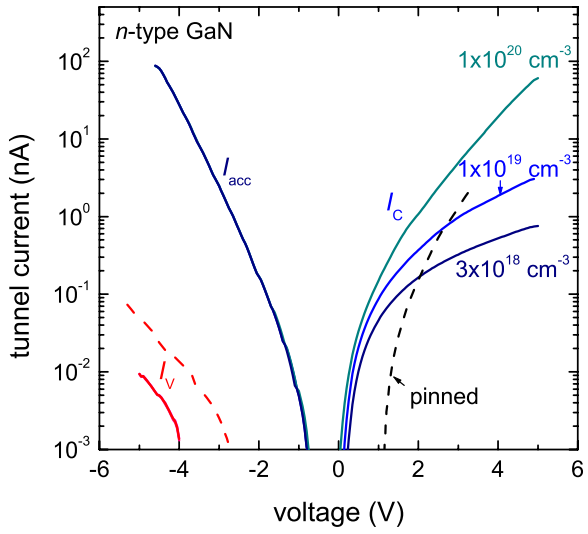

FIG. 4. (Color online) Calculated tunneling currents for the metal tip–vacuum–GaN tunneling junction for three different *n*-type free-carrier concentrations (solid lines, unpinned GaN) and a pinned GaN surface (dashed lines) as a function of the sample bias voltage. I_C denotes the electron current from the tip in to empty conduction-band states of the semiconductor (solid curves at positive voltages). I_{acc} is the tunnel current arising from the electron accumulation in the conduction-band states due to the tip-induced band-bending [upper solid (blue) curves at negative voltages, see schematic in Fig. 1]. I_V denotes the tunnel current from the valence-band states into the tip [lower solid and dashed (red) curves at negative voltages]. Note, the current contributions I_{acc} and I_V are essentially independent of the doping level for unpinned GaN (because the band bending shown in Fig. 2 is at negative voltages independent of the doping level) and thus the respective three curves calculated for the indicated three different doping levels overlap at negative voltages. Note the large domination of the valence-band current I_V by the accumulation current I_{acc} in case of unpinned GaN surfaces. As a result only conduction-band states are visible in scanning tunneling images of unpinned GaN surfaces. The dashed spectrum (marked "pinned") shows the tunnel current originating in the valence (negative voltages) and conduction bands (positive voltages), respectively, calculated for a nonpolar GaN surface pinned by a defect level 1 eV below the conduction-band edge. For pinned GaN no accumulation current exists.

energy values (see Fig. 3) for voltages $V<-0.4$ V. Once this happens, the conduction band can be filled by majority carriers (electrons) and an accumulation zone develops. This accumulation zone has a high density of states and screens the electric field of the tip more efficiently than the doping. As a result the curves of the band edges in Fig. 3 bend. This effect is independent of the doping level. In principal, in an analogous manner, the valence-band maximum can also cross the Fermi energy at large positive voltages for the lower-doped samples and in equilibrium an inversion zone by hole (minority-carrier) accumulation in the valence band could form. However, as shown in Ref. 10 and below here the latter effect cannot persist under tunneling conditions due to the carrier dynamics.

At this stage we discuss, how these additional effects influence the tunnel current. For this purpose we calculated the four different contributions to the tunnel current. Three of the four contributions are shown in Fig. 4: I_C, I_V, and I_{acc}. I_C is the tunnel current into empty conduction-band states. As expected from Fig. 3 it starts around between +0.1 and +0.3 V depending on the doping level. In analogy, I_V is the tunnel current out of filled valence-band states into the empty tip states starting again as expected around −3.9 V. The most interesting contribution to the tunnel current is I_{acc}. It arises from electrons tunneling out of the accumulation zone in the conduction band into empty tip states. Thus, the accumulation current probes the conduction-band states at negative voltages instead of probing filled valence-band states. The accumulation current I_{acc} is four orders of magnitude larger than the valence-band current I_V and it starts already at voltages around −0.75 V almost independent of the doping level. Note, the starting voltage ultimately reaches a value close to −0.4 V if determined for currents $\ll 1$ pA. This is in agreement with the band-edge positions in Fig. 3. As a result, the apparent band gap in tunneling spectra appears only 0.5–0.9 V wide, depending on the tunnel current (i.e., tip-sample separation) used to measure the spectra. Thus, the band-gap determination fails completely for unpinned GaN$(1\bar{1}00)$ surfaces. Furthermore, the accumulation current fully dominates the current at negative voltages and no valence-band current can be reliably distinguished within the total current. Therefore, the STM images will show at positive and negative voltages only contributions originating from conduction-band states. Valence-band states are invisible, independent of the doping concentration. Similarly, the determination of the band-edge positions is hampered.

This is in contrast to GaAs(110) surfaces, where the band gap can be reliably determined following the procedure in Ref. 10. The main differences are twofold. On the one hand, GaAs(110) has an indirect surface band gap. The electrons in the accumulation layer of the conduction band have to tunnel with a nonzero momentum. Since the tunnel effect conserves the momentum the tip has to have states accommodating the momentum. This is mostly not the case and the magnitude of the accumulation current is therefore strongly reduced. In contrast, GaN$(1\bar{1}00)$ has a direct band gap at the $\bar{\Gamma}$ point[7,12] and thus no suppression due to momentum conservation exists. Furthermore the band gap of GaN is much larger than of GaAs. For GaN, this significantly increases the tunneling barrier for tunneling out of valence-band states as compared to tunneling into or out of conduction-band states, reducing even further the valence-band current. Therefore, on unpinned GaN$(1\bar{1}00)$ surfaces no atom-selective imaging is possible, in contrast to GaAs(110).

Note, the fourth contribution to the tunnel current, is the tunneling at large positive voltages into emptied valence-band states of a possible inversion layer. It is not shown in Fig. 4 because it is many orders of magnitude smaller and thus irrelevant. Since a stable tunnel current requires that the valence-band states remain permanently empty under tunneling conditions (i.e., electron injection), the electrons tunneling into the inversion zone needs to be removed from there. This is only possible by (i) hole diffusion from the bulk to the surface or (ii) electron tunneling from the valence to the conduction band. However, both (i) the hole concentration is too small in *n*-type GaN and (ii) the barrier height on the

order of $E_{gap}=3.4$ eV as well as the barrier width between the valence-band maximum at the surface and the conduction-band minimum in the bulk (at equal energy) are too large, due to the extended band bending (see, e.g., inset in Fig. 2). Therefore, both processes cannot maintain a sizable tunnel current. Thus, under tunneling conditions an inversion layer is instantly filled and removed.[10,14]

Finally, there are nevertheless conditions under which one can determine properly the band gap and the band-edge position of the GaN($1\bar{1}00$) surfaces as experimentally shown in Ref. 7. The key to this is the pinning of the GaN($1\bar{1}00$) surface by defects. The pinning of the Fermi energy reduces the band bending and thereby blocks the surface valence-band and conduction-band edges to shift by band bending as for the case of unpinned GaN($1\bar{1}00$) surfaces shown in Figs. 2 and 3. Therefore, no electron accumulation develops in the conduction band and the accumulation current from filled conduction-band states is absent. Under such conditions, the valence-band current I_V is the only current at negative voltages (neglecting defect states) (see red dashed line at negative voltages in Fig. 4). As illustrated by the dashed spectra in Fig. 4 (labeled pinned), for pinned GaN($1\bar{1}00$) surfaces the voltage onsets of I_V and I_C times the electron charge e yields directly the band-edge positions and its difference the size of the band gap, in contrast to unpinned GaN($1\bar{1}00$) surfaces.

IV. COMPARISON WITH EXPERIMENTAL DATA

At this stage we compare our theoretical results with experimental data. The calculations yield that for unpinned nonpolar GaN surfaces only conduction-band states can be probed at positive and negative voltages and the apparent band gap is significantly reduced in scanning tunneling spectra as compared to the real one. As a consequence the apparent band-edge positions cannot be determined in scanning tunneling spectra. In contrast, on pinned nonpolar GaN surfaces, the tunnel current originates from tunneling out of valence-band and into conduction-band states at negative and positive voltages, respectively. Thus, accurate band gaps and band-edge positions can be extracted.

Unfortunately, for a detailed comparison the so far published experimental STS data is limited to GaN($1\bar{1}00$) surfaces pinned by defect states in the band gap.[7] This data on pinned GaN($1\bar{1}00$) surfaces show clearly that valence-band and conduction-band currents can be well distinguished and the band gap as well as the band-edge positions can be extracted accurately. In addition, the experimental data illustrates that the intrinsic surface states are outside the fundamental band gap. Thus, GaN($1\bar{1}00$) surfaces can be unpinned if prepared with a low defect concentration.

Recent unpublished STM and STS data[18] on unpinned GaN($1\bar{1}00$) surfaces (with a lower defect concentration) show, in contrast to pinned surfaces, only conduction-band states at, both, positive and negative voltages. Valence-band states cannot be detected in scanning tunneling spectra measured on unpinned GaN($1\bar{1}00$) surfaces. Furthermore, the apparent size of the band gap in STS data is much smaller than expected for GaN, in agreement with our calculation. The experimental results thus corroborate our calculated tunnel currents and conclusions, in particular, the invisibility of valence-band states on unpinned nonpolar GaN surfaces.

V. CONCLUSIONS

In conclusions, scanning tunneling microscopy images of unpinned n-type GaN($1\bar{1}00$) surfaces show at all voltages only the conduction-band states independent of the doping concentration, due to an electron accumulation in conduction-band states at negative sample voltages. Valence-band states are not detectable because the tunnel current from the accumulation zone in the conduction band is strongly dominating due to lower energy barrier for tunneling in or out of conduction-band states and a direct surface band gap of GaN($1\bar{1}00$). Therefore, the STM images show only the Ga-derived dangling bonds and an atom-selective imaging as well as a band-gap determination are impossible for unpinned GaN($1\bar{1}00$) surfaces. Only for pinned GaN($1\bar{1}00$) surfaces, valence-band states contribute and thus the atom-selective imaging of Ga- and N-derived dangling bonds is possible as well as the determination of the band-gap size in tunneling spectra is accurate.

ACKNOWLEDGMENT

The authors thank the Deutsche Forschungsgemeinschaft for financial support.

*p.ebert@fz-juelich.de

[1] J. Tersoff and D. R. Hamann, Phys. Rev. Lett. **50**, 1998 (1983); Phys. Rev. B **31**, 805 (1985).

[2] R. M. Feenstra, J. A. Stroscio, J. Tersoff, and A. P. Fein, Phys. Rev. Lett. **58**, 1192 (1987).

[3] O. Albrektsen, D. J. Arent, H. P. Meier, and H. W. M. Salemink, Appl. Phys. Lett. **57**, 31 (1990); M. B. Johnson, H. P. Meier, and H. W. M. Salemink, *ibid.* **63**, 3636 (1993).

[4] R. M. Feenstra, Semicond. Sci. Technol. **9**, 2157 (1994).

[5] W. Barvosa-Carter, M. E. Twigg, M. J. Yang, and L. J. Whitman, Phys. Rev. B **63**, 245311 (2001).

[6] P. Waltereit, O. Brandt, A. Trampert, H. T. Grahn, J. Menninger, M. Ramsteiner, M. Reiche, and K. H. Ploog, Nature (London) **406**, 865 (2000).

[7] L. Ivanova, S. Borisova, H. Eisele, M. Dähne, A. Laubsch, and Ph. Ebert, Appl. Phys. Lett. **93**, 192110 (2008).

[8] Ph. Ebert, L. Ivanova, S. Borisova, H. Eisele, A. Laubsch, and M. Dähne, Appl. Phys. Lett. **94**, 062104 (2009); H. Eisele, L.

Ivanova, S. Borisova, M. Dähne, M. Winkelnkemper, and Ph. Ebert, *ibid.* **94**, 162110 (2009).

[9] R. M. Feenstra and J. A. Stroscio, J. Vac. Sci. Technol. B **5**, 923 (1987).

[10] N. D. Jäger, E. R. Weber, K. Urban, and Ph. Ebert, Phys. Rev. B **67**, 165327 (2003).

[11] Thus far, the wave vector of the tunneling electrons have only be measured for the compound semiconductors InP(110) [Ph. Ebert, C. Cox, U. Poppe, and K. Urban, Surf. Sci. **271**, 587 (1992); Ultramicroscopy **42-44**, 871 (1992)] and GaN($1\bar{1}00$) (Ref. 7) using the method of J. A. Stroscio, R. M. Feenstra, and A. P. Fein, Phys. Rev. Lett. **57**, 2579 (1986); However from combined normal and inverse photoemission measurements [H. Carstensen, T. Holdmann, R. Claessen, R. Manzke, and M. Skibowski, Phys. Rev. B **41**, 9880 (1990)] it can be inferred that most III-V zinc-blende type semiconductors have an indirect surface band gap.

[12] J. E. Northrup and J. Neugebauer, Phys. Rev. B **53**, R10477 (1996).

[13] R. Seiwatz and M. Green, J. Appl. Phys. **29**, 1034 (1958).

[14] N. D. Jäger, Ph. Ebert, K. Urban, R. Krause-Rehberg, and E. R. Weber, Phys. Rev. B **65**, 195318 (2002).

[15] J. Bono and R. H. Good, Jr., Surf. Sci. **175**, 415 (1986).

[16] A. Selloni, P. Carnevali, E. Tosatti, and C. D. Chen, Phys. Rev. B **31**, 2602 (1985).

[17] N. D. Jäger, K. Urban, E. R. Weber, and Ph. Ebert, Appl. Phys. Lett. **82**, 2700 (2003).

[18] P. Löptien and M. Wenderoth, Spring Meeting of the German Physical Society, March 23–27, 2009.